Faraday Discussions

Accepted Manuscript

This manuscript will be presented and discussed at a forthcoming Faraday Discussion meeting. All delegates can contribute to the discussion which will be included in the final volume.

Register now to attend! Full details of all upcoming meetings: http://rsc.li/fd-upcoming-meetings

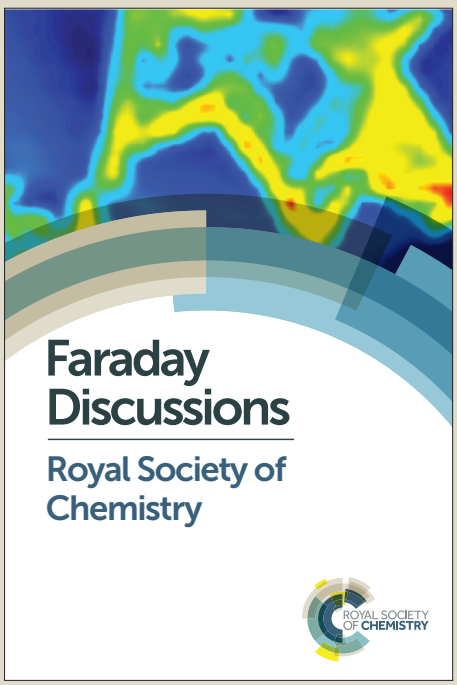

This is an *Accepted Manuscript*, which has been through the Royal Society of Chemistry peer review process and has been accepted for publication.

Accepted Manuscripts are published online shortly after acceptance, before technical editing, formatting and proof reading. Using this free service, authors can make their results available to the community, in citable form, before we publish the edited article. We will replace this *Accepted Manuscript* with the edited and formatted *Advance Article* as soon as it is available.

You can find more information about *Accepted Manuscripts* in the Information for Authors.

Please note that technical editing may introduce minor changes to the text and/or graphics, which may alter content. The journal's standard Terms & Conditions and the Ethical guidelines still apply. In no event shall the Royal Society of Chemistry be held responsible for any errors or omissions in this *Accepted Manuscript* or any consequences arising from the use of any information it contains.

ROYAL SOCIETY OF CHEMISTRY

www.rsc.org/faraday_d

CREATED USING THE RSC REPORT TEMPLATE (VER. 3.1) - SEE WWW.RSC.ORG/ELECTRONICFILES FOR DETAILS
PAPER Faraday Discussions www.rsc.org/xxxxxx | XXXXXXXX

Measurement and control of detailed electronic properties in single molecule break junction

Kun Wang, Joseph Hamill, Jianfeng Zhou, Cunlan Guo, and Bingqian Xu *

DOI: 10.1039/b000000x [DO NOT ALTER/DELETE THIS TEXT]

The lack of detailed experimental controls has been one of the major obstacles that hinder the progress in molecular electronics. While experimental data remains all over the map, specific details, related mechanisms, and data analysis techniques are in high demand to promote our physical understanding at the single-molecule level. A series of modulations we recently developed based on traditional scanning probe microscopy break junction (SPMBJ) have helped to discover significant detailed properties hidden in the contact interfaces of a SMBJ. For example, in the past we have shown that the correlated force and conductance changes under the saw tooth modulation and stretch-hold mode of PZT movement revealed inherent differences in contact geometries of a molecular junction. In this paper, using bias modulated SPMBJ and utilized emerging data analysis techniques, we report on the measurements of altered alignment of the HOMO of benzene molecules when we changed the anchoring group which coupled the molecule to metal electrodes. Further calculations based on Landauer fitting and transition voltage spectroscopy (TVS) demonstrated the effects of modulated bias on the location of the frontier molecular orbitals. Understanding the alignment of the molecular orbitals with the Fermi level of the electrodes is essential for understanding the behaviour of SMBJs and for the future design of more complex devices. With these modulations and analysis techniques, fruitful information has been found about the nature of the metal-molecule junction，providing us insightful clues for the next step for in-depth study.

Introduction

Since it was conceived, the concept of molecular electronics started with the idea of wiring an individual molecule to two metal electrodes as an analogy of single electronic components in commercial microelectronic devices.[1, 2] Stimulated by the high degree of diversity and functionality of molecules and the nanometre scale dimension of this system, both experimental and theoretical investigations in this direction have been in steady progress for more than two decades, although with many obstacles.[3-11] Among techniques enabling the sandwiching of an individual molecule between two electrodes, single-molecule break junction (SMBJ) provides a robust and tuneable platform to probe inherent properties and gain fundamental understanding of molecular-scale electronic elements.[10, 12] The key feature lies with the electronic transport properties of a SMBJ.

A SMBJ is a simple yet very complex system. To depict the simplicity, a SMBJ only consists of two parts: a nanoscopic molecule and two macroscopic electrodes.

Multiple metal materials have been studied as the SMBJ electrodes, such as Au, Pt, Ag and Pd. [7, 13-15] Similarly, molecular species spanning from simple saturated molecules[16-18] to intricate conjugated molecules[19-22] have been tested for various purposes. Within a SMBJ the metal electrodes consist of a very condensed set of continuous energy states, the Fermi level of which varies from material to material, but the isolated molecule in the center of the junction contains a discrete set of energy levels, with a highest-occupied (HOMO) and a lowest unoccupied molecular orbital (LUMO). This last quality is what distinguishes SMBJs from classical p-n junctions which can be modelled with continuous bands throughout. Bridging an individual molecule between two metal electrodes leads to the broadening of discrete energy levels causing a quasicontinuum density of states due to the hybridization with the metal wave functions. In other words, the charge transport properties across a SMBJ are essentially determined by the alignment of continuous electrode energy levels and discrete molecular energy levels. The interface connecting the molecule and electrodes is the source of the complexity of a SMBJ system. Unlike in a semiconductor system where the contact parts are ignored because of their Ohmic behaviour, the contact interfaces in a SMBJ have a strong influence, and sometimes even dominate the electron transport. Apart from the electrodes, chemical ligands, the other factor involved in the interfaces which is used to wire a molecule to the electrodes, have been widely studied. These include amines (-NH_2), thiols (-SH), carboxyls(–COOH), dimethyl phosphines (–PMe_2) and, recently selenols (–SeH).[23-29] The environment where electrical measurements are conducted, often in a liquid buffer, also has a non-negligible impact on the properties of a SMBJ.[30, 31] Especially for DNA molecules, this influence is critical.[32, 33]

Challenges emerge in both experiments and simulations. Since experimental data always reflect a mixed result of various effects that get involved in a SMBJ system, it is necessary to elaborately define each factor that may influence the final result. Without enough understanding of them, no conclusion can be drawn convincingly. Experimental difficulties rest with how to control those factors separately and explore them one by one at the scale far beyond human eyesight. Similarly, development in simulations is limited by the size of the system and oversimplification.[34] Even so, great efforts have been made experimentally and theoretically to date.[10, 35-41] Investigations into different combinations of molecules and electrodes, and multiple controls of contact effect and environmental conditions have been reported over the past decade.[42-44] To clear the mists above this field, researchers are driven to keep innovating experimental designs and simulation methods. We have been focusing on experimental modulations and designs using the SPMBJ technique in order to gain deep insight towards a comprehensive understanding of the whole SMBJ system. In the following, we will briefly discuss our previous work in tuning the measurement process, and report on the controls of contact interfaces and relevant theoretical analysis.

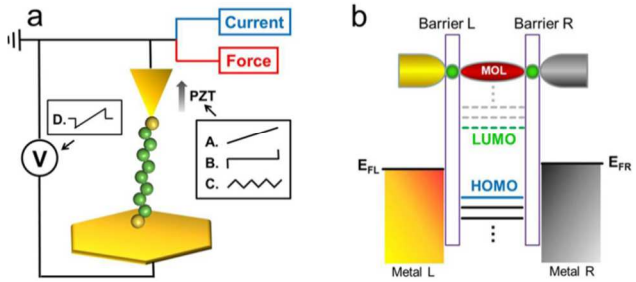

Figure 1. (a) Schematic of SPMBJ setup. Continuous-stretch A, stretch-hold B, and saw tooth C are possible PZT displacement modulation modes. D is a possible bias modulation mode. (b) Energy profiles of a SMBJ including the continuous energy states of metal electrodes and discrete energy levels of the molecule (HOMO in solid blue and LUMO in dashed green).

Results and Discussion

1. Experimental modulations

This section will briefly discuss multiple experimental modulations we previously developed and the detailed electrical and mechanical properties discovered by using these modified techniques.

The power of the SPM (STM/CAFM) experimental setup comes from the flexibility it offers the experimentalist: 1) The piezoelectric transducer (PZT) provides precise displacement of the SPM tip, allowing for the gap between the tip and substrate to be adjusted continuously (A, B and C modulation modes in Fig. 1a); and 2) The SPM allows for a bias to be applied and modulated between the tip and substrate (D modulation mode in Fig. 1a). Both of these variables can be controlled by a computer program and a feedback mechanism.

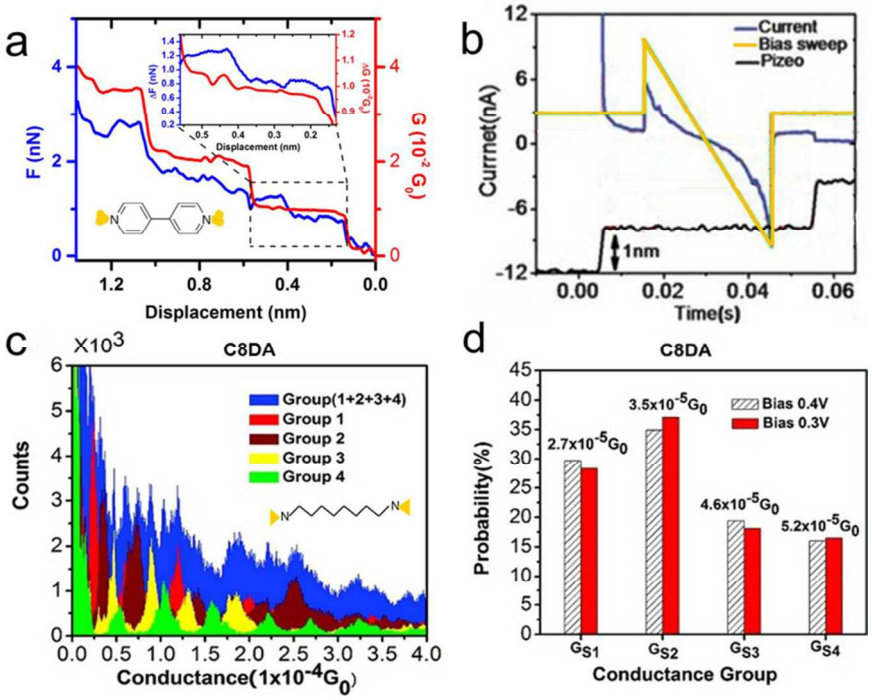

Figure 2. (a) Continuous-stretch mode force (blue) and conductance (red) traces from 4,4'-bipyridine SPM break junctions showing quantized steps for 1, 2, and 3 conducting molecules in the junction. (b) Black curve is the displacement of the PZT during stretch-hold mode; green curve is the applied bias modulation during the step of the stretch-hold modulation; blue is the induced current when the bias across the molecule is swept from 1V to -1V. (c) Conductance histograms from C8DA SPM break junctions showing four different sets of conductance. (d) Conductance values measured under 0.3V and 0.4V for the four sets in (c). (c) and (d) are reprinted from ref. 47.

1.1 Continuous-stretch mode The first experiments using the SPM design created an ensemble of transient junctions by rapidly and repeatedly approaching the tip to the substrate, and retracting it in a continuous motion, controlled by the PZT.[10] The conductance of the junction during the retraction phase revealed first quantized Landauer steps[45] corresponding to the Au-Au junction, and once the final Au-Au junction broke, quantized steps caused by individual molecules in the junction (Fig. 2a). This second set of quantized steps in the conductance was associated with one molecule, two molecules, etc. present in the junction. The introduction of this technique resolved most discrepancies caused by the defective formation of molecular junctions.

1.2 Dual-mode feedback At the single-molecule level, one of the difficulties in experimental measurements is to maintain complete molecular junctions over thousands of repeated measurement processes. In order to achieve multiple electromechanical modulations but still keep the junction system intact enough, we developed a comprehensive controlling system.[46] With a dual-mode feedback control on traditional CAFM techniques, this highly integrated SPM system realized the tuneable contact strength and many other modulations. Based on this system, the tip was first controlled by the "current-feedback" mode due to its high sensitivity to tip-substrate separation. However, the possible peeling of the conductive coating on the

tip which results in decreased conductance may blind the engaging process by pushing the tip until the limit of the PZT, which in most cases will crash the CAFM tip. At the core of our design is that the system normally runs under the "current-feedback" mode, but if the current exceeds a higher current set point, the system will automatically switch to the "force-feedback" mode to avoid the crashing of the CAFM tip. If the current resumes, the system can automatically turn back to "current-feedback." The experimental tests on octanedithiol (C8DT) molecules proved the robustness of this system.

1.3 Stretch-hold mode The steady linear retractions of continuous-stretch mode SPM measurements created single molecular junctions across which single molecular conductance was measured, but the junctions were short lived and the histograms missed significant details important for understanding the SMBJ systems it was measuring. The solution was to stair-step the retraction process as B modulation mode in Fig. 1a shows so that the system paused momentarily and allowed for the junction to settle into a quasi-relaxed state.[47] This allows one to eliminate, or at least minimize, the variations of experimental conditions. The retraction-pause-retraction was controlled by a computer program prescribing the displacement of the PZT controlling the SPM tip.

1.4 Bias modulation mode When the stretch-hold mode SPM pauses during retraction, it provides a unique opportunity for the molecule to be perturbed while in a quasi-steady state junction. For example, the bias can be swept through a range of values to create an I-V curve similar to those used to study other electronic devices.[48] Fig. 2b shows a typical I-V curve responding to the bias sweep applied on a stretch-hold mode single-molecule conductance plateau. The characteristics of the I-V can reveal information about the symmetry of the junction and the molecular orbitals within the junction. Indeed, one of the first goals of created SMBJs was to create rectifying asymmetric single molecular junctions.[1] Since then it has been shown that even geometrically symmetric junctions can show rectifying behaviour in SPM break junctions.

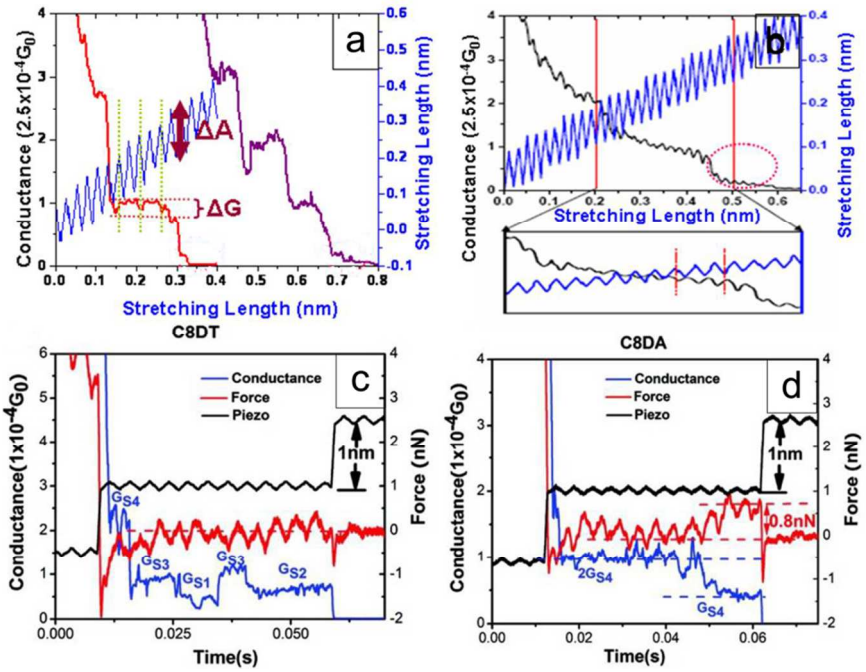

Figure 3. Representative traces indicating various specific characteristic features. The conductance traces of C8DT under the saw-tooth modulations on continuous retraction process show a correspondent conductance fluctuation of ΔG (a) and out-of-phase (180° phase shift) correspondence to the modulation (b). (c) and (d) show the conductance and force traces under the saw tooth modulation applied on stretch-hold mode. (c) The trace with conductance switching between different single molecular conductance sets but without obvious force change in force. (d) The trace with conductance changes with dissociations of molecules from electrodes caused by the contact bond broken, GS1−GS4 (C8DT, 4.8×10^{-5}, 7.0×10^{-5}, 9.0×10^{-5}, and 24.9×10^{-5} G_0) in (c) and GS4 (C8DA, 5.2×10^{-5} G_0) in (d) are the single molecular conductance sets reported in ref. 47. (a) is reprinted from ref. 49. (c) and (d) are reprinted from ref. 50.

1.5 Saw tooth modulations The displacement of the SPM tip as it is retracted from the surface can be controlled in numerous ways, limited only by the programmability of the PZT in control of the tip. Besides the stretch-hold modulation, the tip can also be induced to cycle through saw tooth displacements while it is being retracted. In one cycle, the tip performs a compress followed by an elongation movement. Modulations in this manner influence the specific geometric orientation of the molecule with the electrodes and therefore alter the conductance histograms. The SPM mechanism can be modified to measure force simultaneously with conductance using a conducting CAFM, and when this saw tooth modulation was applied to CAFM SPM measurements, the effects of the contact geometry and bond distance were isolated in the conductance signal.

1.6 Detailed properties Using the modulations described above, we have discovered significant detailed properties of a SMBJ. The stretch-hold mode conductance histograms yielded much finer peaks and also successfully identified the small variation due to the molecule-electrode contact configuration differences of Au-C8DT/C8DA-Au molecular junctions (Fig. 2c and 2d). The saw tooth modulation applied on the continuous-stretch mode conductance measurements revealed regular fluctuations (Fig. 3a) on the

conductance traces with a 180° phase shift (Fig. 3b) in relation to the PZT modulation. The saw tooth modulation applied on the free-holding process of the stretch-hold mode measurements of Au-C8DT/C8DA-Au illustrated more detailed phenomena: 1) conductance switching between different conductance sets were observed on some conductance traces (Fig. 3c), which is suggested to be caused by the switching among different adsorption sites of Au atoms induced by the mechanical modulation; 2) for C8DA, the conductance switching accompanied with a force change close to the Au-NH_2 binding force strongly suggested that the responsive conductance changes are a combination of the switching between different adsorption sites and the dissociation of the molecule from the electrode with the bond broken under modulations (Fig. 3d). In addition, using the bias modulation, single molecule junctions composed of a thiol-terminated Ru(II) bis-terpyridine (Ru(tpy-$SH)_2$) molecule sandwiched between two gold electrodes was observed to have a contact-specific NDR at positive low-bias range.[48] NDR was observed to occur only for hollow-top Au-S binding configuration. Differential conductance profiles showed extra peaks which we suggested to be caused by small HOMO-LUMO gap and hybridization among the transition metal center, organic molecule backbone and Au electrodes. Simultaneous force measurements suggested the bias-induced molecule-electrode coupling change as the major cause. In such a strong coupled molecular junction, we proposed that the specific contact configuration dominated the NDR effect.

1.7 Barrier model To understand the experimental phenomena observed under applied mechanical modulations, we established a modified multiple tunneling barrier model incorporating a contact resistance term (Fig. 4).[49] In this model, the molecule core was defined as a rigid body which remained intact under junction extension Δd. The extension parameter Δd is to simulate the elongation movement of the tip in the saw tooth modulation. The molecule–electrode contacts were considered as a rectangular potential barrier where the contact decay constant βc (the height of the potential barrier) and the width of the potential barrier d were used as two crucial indices to describe the effects of contact conformation change. Thus, the final conductance $G=A\times exp(-\beta_M)\times exp(-\beta_C)$. Using this model, we identified the static contact resistances for stable C8DT and C8DA molecular junctions, which were divided into four conductance sets. By monitoring the decay constant changes and force changes under mechanical modulation/extensions, we found that they changed differently not only with molecule–electrode contact bonds (Au–S and Au–NH_2) but also with their conductance sets.

These experimental modulations and theoretical models have either yielded new detailed phenomena or further improved existed theories, providing fresh physical understanding about the missing essence of a molecular junction.

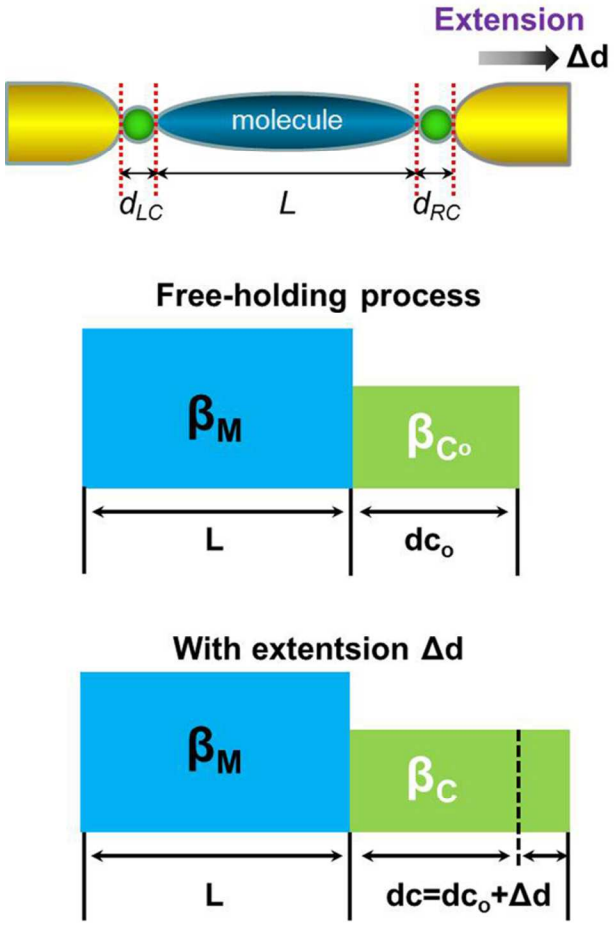

Figure 4. Modified multiple tunneling barrier models.

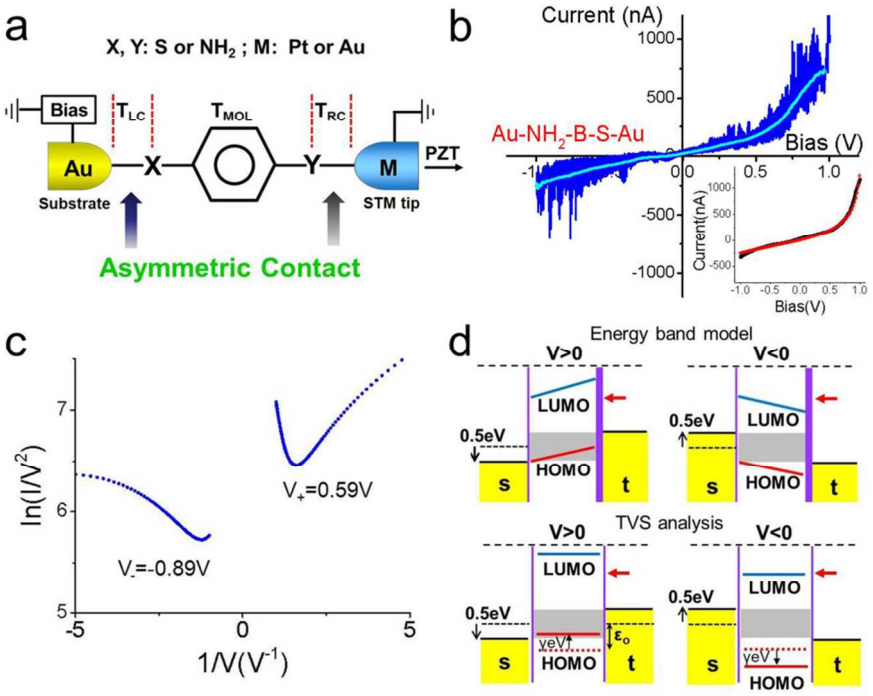

Figure 5. (a) Schematic of Benzene-based molecular junctions with changeable electrodes and anchoring groups; (b) I-V characteristics and Landauer fitting (inset red curve) of Au-NH_2-B-S-Au junction; (c) $\ln(I/V^2)$ vs 1/V plot for I-V curves in (b), transition voltages (V_+ and V_-) were labeled; (d) Energy band model and TVS analysis schematics

2. Controls of contact variables

In this section we will present the new experimental measurements in controlling the contact effect and the relevant data analysis.

As the bias-sweep modulation on the stretch-hold mode SPMBJ enables us to study the I-V characteristics of a single-molecule junction, the I-V characteristics of potential functional molecular devices, like molecular rectifiers, are our main focus. One of the less-understood issues in rectification behaviour of a SMBJ is the role of contact interfaces. To gain insights into the rectification behaviour induced by asymmetric contacts in a SMBJ, we performed a comprehensive investigation of the charge transport properties of molecular junctions with systematic controls on both anchoring groups and electrodes (Fig. 5a). Combining the stretch-hold and bias sweep modification of SPMBJ, I-V characteristic were measured for molecules consisting of a central benzene ring (B), alternating anchoring groups of thiol (-SH) and amine (-NH_2). The electrodes consist of a Au substrate and a STM tip which alternates between Au and Pt. In total, five different molecular junctions were measured. Due to the symmetric and rigid inherent structure of the benzene ring, any asymmetric electronic behaviour should come from the two contacts. As the experimental result revealed, pronounced rectification behaviour occurred when an asymmetric component, an asymmetric anchoring group, an asymmetric electrode, or both in combination, was introduced into the molecular junction. Example I-V curves for Au-NH_2-B-SH-Au junction are shown in Fig. 5b. Using an energy band model,[50] where molecular orbital at the strong coupled contact tends to shift together

with the chemical potential of corresponding electrode, rectification was accessed due to the asymmetric shift of molecular frontier orbitals with respect to Fermi levels of the electrodes, which resulted from the coupling strength asymmetry at two contact interfaces (Fig. 5d). Comparing the binding energies of different anchoring group-electrode combinations,[14, 51] the differences in coupling strength were determined. It turned out that our experimental results agreed well with the prediction of the energy band model. The degree of asymmetry of the coupling strength at two contacts determined the rectification ratio of the molecular junction. For example, Au-NH_2-B-SH-Pt junction which possesses the most asymmetric contact coupling strength should have the largest rectification ratio. It was accordant with our experimental results. Otherwise, we believe that the external bias played a significant role in triggering the rectifying behaviour.

2.1 I-V Curve Calculations

Possibly the most valuable information that experimentalists hope to discover using SMBJs is the energy gap between the Fermi level of the electrodes and the nearest conducting orbital of the molecule in the break junction. This parameter determines the turn-on voltage necessary to yield a high current in a molecular electronics device. This orbital is either the HOMO or LUMO, and usually the Fermi level of the electrodes is closer to one or the other, which means when a bias is applied, the nearest one is reached first, resulting in a drastic increase in conductance. However, experimental junctions often break down before this voltage can be reached, so the energy gap must be derived from more circuitous methods. Two such methods are easily calculated from the I-V curves measured from bias-modulated mode SMBJs. Each method has strengths and weaknesses.

2.1.1 I-V curve fitting An I-V curve can be fit to a simplified version of the Landauer formula, involving only three fitting parameters, using a Levenberg-Marquardt least squares fitting algorithm.[52] The three parameters correspond to the gap ε_{fit} described above, and the degree of coupling, Γ_L and Γ_R, to each electrode separately. When this fitting method was applied to the five different junctions with variable anchoring groups and electrodes, the results agreed with observations made from the qualitative analysis of the I-V curves. The symmetric junctions yielded symmetric values for Γ_L and Γ_R, and yielded unequal values when the junctions were asymmetric (see Table 1). This provides a quantitative confirmation for the observation that the asymmetric junctions yielded asymmetric I-V curves due to unequal coupling to the molecule. Furthermore, the energy levels when Pt was used as one of the electrodes, was considerably altered compared to Au-molecule-Au junctions.

Table 1 Landauer Fitting and TVS analysis results for different molecular junctions

Molecular Junction[a]	Landauer Fitting			TVS	
	Γ_L (eV)	Γ_R (eV)	ε_{fit} (eV)	ε_{TVS} (eV)	γ
Au-S-B-S-Au	7.63E-4	7.69E-4	0.71	0.61	-0.01
Au-NH_2-B-NH_2-Au	3.11E-4	3.18E-4	0.71	0.69	-0.01
Au-NH_2-B-S-Au	3.19E-4	6.60E-4	0.87	0.62	-0.06
Au-S-B-S-Pt	5.89E-4	7.10E-4	0.75	0.49	-0.03
Au-S-B-NH_2-Pt	1.15E-3	5.09E-4	0.92	0.57	0.08

[a] Molecular junctions in the first column are expressed in the format of substrate-molecule-tip.

2.1.2 Transition voltage spectroscopy (TVS) Yet another interpretation of the

Landauer formula yields information about the energy gap ε_{TVS} of the SMBJ from a Fowler-Nordheim (FN) plot of the I-V curve. Specifically, a FN plot of an I-V curve measured from a SMBJ can yield minima at specific transition voltages (Fig. 5c). The corresponding bias voltage at a specific minimum indicates the transition voltage where a trapezoid shaped tunneling barrier turns to a triangle shaped barrier. It is necessary to notice that this transition voltage is different from the bias voltage enabling the alignment of the frontier molecular orbital of the molecule with the chemical potential of the metal electrodes. Namely, the transition voltage is smaller than the voltage potential necessary for a resonant tunneling. Using these minima, it is possible to calculate the energy gap between the Fermi level of the electrodes and the nearest conducting molecular orbital, and a coefficient γ which determines the degree of relative shift of the nearest molecular orbital under a certain bias.[6, 53] By comparing these two core parameters, ε_{TVS} and γ, we found: 1) comparing Au-SH-B-SH-Au and Au-NH_2-B-NH_2-Au junctions, the latter has a bigger ε_{TVS} but smaller γ which resulted in lower current within the applied bias range. As the binding energy calculation suggested, this difference should be a result of the difference between Au-SH and Au-NH_2 contact bonds. 2) Comparing Au-SH-B-SH-Au and Au-NH_2-B-SH-Au, when an asymmetric anchoring group (weaker coupling Au-NH_2 bond) was introduced, ε_{TVS} becomes larger, but a greater γ effect was also introduced. Noticeably, ε_{TVS} for the Au-NH_2-B-SH-Au junction is between that of Au-SH-B-SH-Au and Au-NH_2-B-NH_2-Au junctions, suggesting it to be a hybridization of those two junctions. 3) Comparing Au-SH-B-SH-Pt with Au-SH-B-SH-Au, when an asymmetric electrode component was introduced, the whole system was altered since the Fermi level of one electrode offsets from that of the other. ε_{TVS} becomes much smaller and γ almost doubles. The smaller ε_{TVS} of Au-SH-B-SH-Pt could be caused by the asymmetric Fermi level at the two electrodes. 4) For junction Au-SH-B-NH_2-Pt, it has a similar ε_{TVS} compared to the Au-SH-B-SH-Au junction although these two junctions are based on two different molecules, which suggests a similar bonding strength between Au-SH and Pt-NH_2, confirmed by previous binding energy calculation. This junction has the biggestγ, which is believed to be the main reason for the rectification behavior observed at negative bias (see Table 1).

Overall, based on TVS, whenever an asymmetric component was introduced it increased the value of γ, intensifying the degree of HOMO relative shift. Thus, it is possible that the frontier molecular orbital shifted into the transmission window or the field emission transport was induced under high bias. Besides, when Pt electrode was involved, the ε_{TVS}energy offset becomes smaller (the results from the Landauer fit, namely ε_{fit}, do not display this behavior—this will be discussed in the following paragraph), which could be induced by the asymmetric Fermi level position of Au and Pt. Compared with the concept of strong affinity between frontier molecular orbital and electrode Fermi described in the energy band model, the γ value introduced in TVS analysis could be understood in a similar way. Take junction Au-NH_2-B-SH-Au for example (Fig. 4d). Based on TVS, the relative shift of frontier molecular orbital always tries to catch up with the movement of chemical potential of the electrode at the strong coupling interface, which results in the sharp current increase under high positive bias.

To yield precise calculation results from experimental data, theoretical calculations like Landauer fitting and TVS analysis often require smooth and rather pronounced rectifying I-V curves which rarely occur in the bias range where reasonable electrical signal is obtained in real experiments. This could be the major

reason why different calculation algorithms gave different results. Another reason lies with the difficulty in obtaining well-defined minima in the TVS plot. For instance, the ill-defined minimum at the negative bias regime in Fig. 5c may bring more calculation error than the well-defined minima under the positive bias. The common feature the two calculation methods suggested is that resonant tunneling was not reached within our bias sweep range (-1~1V) and the asymmetric coupling, an asymmetric $\Gamma's$ in Landauer fitting and an asymmetric large γ in TVS, is responsible for the resulting rectification I-V characteristics. Both methods rely on simplifications to theoretical models for SMBJs, and therefore do not provide highly accurate results. Their value rests in the relative ease at which important parameters can be calculated from experimental data. Furthermore, the length dependence and effects of screening have been documented for TVS which represent some of the uncertainty in the results of the TVS analysis.[54] However, it is possible this length dependence provides more, not less, information about the details of the conducting molecular orbitals.[55] On the other hand, the results from a Landauer fit are uncertain because any theoretically derived Landauer formula relies on many more variables than coupling strength γ and energy gap ε_{fit}. The simplifications needed to provide a functional form with a limited number of parameters necessitates that the results be interpreted with this in mind: the value of the Landuaer fit is the relative ease at which it can be applied, and the importance of the parameters it yields, not the precision of the results. Precision is still best provided by more complicated simulation methods.

Further experimental and theoretical efforts are needed to test and complete our proposed mechanisms concluded from the responsive experimental signals towards detailed controls as just reported.

Conclusions

Expected as the revolutionary technology for next generation electronic devices, molecular electronics are currently at a fledging stage. To date, only a tiny section of this field has been touched using the existing techniques. We have explored the responses of electronic properties of a molecular junction to multiple mechanical and electrical modulations and used recently developed data analysis techniques to calculate important physical parameters from the data. The experimental results reflect the inherent impact of the contact interface of the electrode and molecule, which is probably the most critical factor in a SMBJ. We have shown that, by tuning the contact distance for alkane molecules, responsive changes in force and conductance indicated the essential difference in contact configurations, which was also explained using a modified multiple tunneling barrier model. By controlling the anchoring groups coupling the molecule to the electrode and the electrodes themselves, we significantly altered how the HOMO of benzene relate to the conductance band of Au electrodes. Specifically, we have shown that the most dramatic effect to the I-V characteristics of a SMBJ occur with a combination of asymmetric electrodes and asymmetric end groups. In this case, the change in HOMO and electrode Fermi level gap is significant, but the most dramatic effect is in the relative shift of the HOMO due to the modulation in the bias.

However, thorough physical and chemical understanding of the electronic properties of a SMBJ requires finer controls which could minimize the influences from most of irrelevant factors, and more advanced data analysis techniques. For

example, careful control of orientations of the molecule sandwiched between the electrodes could provide essential information.[56] Towards this direction, experimental attempts have been made using molecules consisting of benzene rings,[57, 58] but obviously more are needed. Similarly, the fabrication and characterization of molecular junctions with the third gate electrode are of critical significance. From simulation point of view, methods enabling the simulation of long and complex molecules and calculations requiring less simplification and assumptions will provide more precise prediction and constructive guidance for experimentalists.

Although an individual molecule could perform as a conductor, the produced current is far less than what is required for commercial use. Challenges exist in improving and amplifying the current. Doping special chemicals, metal ions and nanoparticles into individual molecules have been suggested to effectively increase the conductivity of a SMBJ. Attempts towards this direction have just started.

Other physical properties involved in a molecular junction like optoelectronics,[59, 60] thermoelectrics,[61, 62] spintronics[63-65] and quantum interference[40] deserve more attention. The responsive signal from them may inspire novel experimental designs and activate fire-new research branches.

Acknowledgement

The authors thank the U. S. National Science Foundation for funding this work (ECCS 0823849, ECCS 1231967).

Notes and References

[a] *Single Molecule Study laboratory, College of Engineering and Nanoscale Science and Engineering Center, University of Georgia, Athens, GA 30602, USA. Email: bxu@engr.uga.edu*

1. A. Aviram and M. A. Ratner, *Chem. Phys. Lett.*, 1974, 29, 277-283.
2. R. L. Carroll and C. B. Gorman, *Angew. Chem., Int. Ed.*, 2002, 41, 4378-4400.
3. A. Nitzan and M. A. Ratner, *Science*, 2003, 300, 1384-1389.
4. J. C. Love, L. A. Estroff, J. K. Kriebel, R. G. Nuzzo and G. M. Whitesides, *Chem. Rev.*, 2005, 105, 1103-1169.
5. N. J. Tao, *Nature Nanotech.*, 2006, 1, 173-181.
6. J. M. Beebe, B. Kim, J. W. Gadzuk, C. D. Frisbie and J. G. Kushmerick, *Phys. Rev. Lett.*, 2006, 97.
7. C. Li, I. Pobelov, T. Wandlowski, A. Bagrets, A. Arnold and F. Evers, *J. Am. Chem. Soc.*, 2008, 130, 318-326.
8. C. Toher, I. Rungger and S. Sanvito, *Phys. Rev. B*, 2009, 79, 205427.
9. H. Dalgleish and G. Kirczenow, *Nano Lett.*, 2006, 6, 1274-1278.
10. B. Q. Xu and N. J. Tao, *Science*, 2003, 301, 1221-1223.
11. C.-C. Kaun and T. Seideman, *Phys. Rev. B*, 2008, 77.
12. R. H. M. Smit, Y. Noat, C. Untiedt, N. D. Lang, M. C. van Hemert and J. M. van Ruitenbeek, *Nature*, 2002, 419, 906-909.
13. C. M. Kim and J. Bechhoefer, *J. Chem. Phys.*, 2013, 138.
14. M. Kiguchi, S. Miura, T. Takahashi, K. Hara, M. Sawamura and K. Murakoshi, *J. Phys. Chem. C*, 2008, 112, 13349-13352.
15. J. M. Beebe, B. Kim, C. D. Frisbie and J. G. Kushmerick, *ACS Nano*, 2008, 2, 827-832.
16. X. D. Cui, A. Primak, X. Zarate, J. Tomfohr, O. F. Sankey, A. L. Moore, T. A. Moore, D. Gust, G. Harris and S. M. Lindsay, *Science*, 2001, 294, 571-574.
17. V. B. Engelkes, J. M. Beebe and C. D. Frisbie, *J. Am. Chem. Soc.*, 2004, 126, 14287-14296.

18. M. A. Reed, C. Zhou, C. J. Muller, T. P. Burgin and J. M. Tour, *Science*, 1997, 278, 252-254.
19. R. E. Holmlin, R. Haag, M. L. Chabinyc, R. F. Ismagilov, A. E. Cohen, A. Terfort, M. A. Rampi and G. M. Whitesides, *J. Am. Chem. Soc.*, 2001, 123, 5075-5085.
20. E. G. Emberly and G. Kirczenow, *Phys. Rev. B*, 2001, 64.
21. S. H. Choi, B. Kim and C. D. Frisbie, *Science*, 2008, 320, 1482-1486.
22. S. O. Kelley, N. M. Jackson, M. G. Hill and J. K. Barton, *Angew. Chem., Int. Ed.*, 1999, 38, 941-945.
23. L. Venkataraman, J. E. Klare, I. W. Tam, C. Nuckolls, M. S. Hybertsen and M. L. Steigerwald, *Nano Lett.*, 2006, 6, 458-462.
24. W. Haiss, S. Martin, E. Leary, H. van Zalinge, S. J. Higgins, L. Bouffier and R. J. Nichols, *J. Phys. Chem. C*, 2009, 113, 5823-5833.
25. R. J. Nichols, W. Haiss, S. J. Higgins, E. Leary, S. Martin and D. Bethell, *Phys. Chem. Chem. Phys.*, 2010, 12, 2801-2815.
26. M. Kamenetska, M. koentopp, A. C. Whalley, Y. S. Park, M. L. Steigerwald, C. Nuckolls, M. S. Hybertsen and L. Venkataraman, *Phys. Rev. Lett.*, 2009, 102.
27. E. Adaligil, Y.-S. Shon and K. Slowinski, *Langmuir*, 2010, 26, 1570-1573.
28. Y. S. Park, A. C. Whalley, M. Kamenetska, M. L. Steigerwald, M. S. Hybertsen, C. Nuckolls and L. Venkataraman, *J. Am. Chem. Soc.*, 2007, 129, 15768-+.
29. F. Chen, X. Li, J. Hihath, Z. Huang and N. Tao, *J. Am. Chem. Soc.*, 2006, 128, 15874-15881.
30. D. P. Long, J. L. Lazorcik, B. A. Mantooth, M. H. Moore, M. A. Ratner, A. Troisi, Y. Yao, J. W. Ciszek, J. M. Tour and R. Shashidhar, *Nature Mater.*, 2006, 5, 901-908.
31. V. Fatemi, M. Kamenetska, J. B. Neaton and L. Venkataraman, *Nano Lett.*, 2011, 11, 1988-1992.
32. R. N. Barnett, C. L. Cleveland, A. Joy, U. Landman and G. B. Schuster, *Science*, 2001, 294, 567-571.
33. Y. A. Mantz, F. L. Gervasio, T. Laino and M. Parrinello, *Phys. Rev. Lett.*, 2007, 99.
34. S. M. Lindsay and M. A. Ratner, *Adv. Mater.*, 2007, 19, 23-31.
35. M. Brandbyge, J. L. Mozos, P. Ordejon, J. Taylor and K. Stokbro, *Phys. Rev. B*, 2002, 65.
36. Y. Selzer, L. T. Cai, M. A. Cabassi, Y. X. Yao, J. M. Tour, T. S. Mayer and D. L. Allara, *Nano Lett.*, 2005, 5, 61-65.
37. F. Chen, J. He, C. Nuckolls, T. Roberts, J. E. Klare and S. Lindsay, *Nano Lett.*, 2005, 5, 503-506.
38. I. Diez-Perez, J. Hihath, Y. Lee, L. Yu, L. Adamska, M. A. Kozhushner, I. I. Oleynik and N. Tao, *Nature Chem.*, 2009, 1, 635-641.
39. H. Vazquez, R. Skouta, S. Schneebeli, M. Kamenetska, R. Breslow, L. Venkataraman and M. S. Hybertsen, *Nature Nanotech.*, 2012, 7, 663-667.
40. C. M. Guedon, H. Valkenier, T. Markussen, K. S. Thygesen, J. C. Hummelen and S. J. van der Molen, *Nature Nanotech.*, 2012, 7, 304-308.
41. M. Taniguchi, M. Tsutsui, R. Mogi, T. Sugawara, Y. Tsuji, K. Yoshizawa and T. Kawai, *J. Am. Chem. Soc.*, 2011, 133, 11426-11429.
42. M. Kiguchi and S. Kaneko, *Phys. Chem. Chem. Phys.*, 2013, 15, 2253-2267.
43. C. Jia and X. Guo, *Chem. Soc. Rev.*, 2013, 42, 5642-5660.
44. R. L. McCreery, H. Yan and A. J. Bergren, *Phys. Chem. Chem. Phys.*, 2013, 15, 1065-1081.
45. V. Rodrigues, T. Fuhrer and D. Ugarte, *Phys. Rev. Lett.*, 2000, 85, 4124-4127.
46. F. Chen, J. Zhou, G. Chen and B. Xu, *IEEE Sens. J.*, 2010, 10, 485-491.
47. J. Zhou, F. Chen and B. Xu, *J. Am. Chem. Soc.*, 2009, 131, 10439-10446.
48. J. Zhou, S. Samanta, C. Guo, J. Locklin and B. Xu, *Nanoscale*, 2013, 5, 5715-5719.
49. J. Zhou, C. Guo and B. Xu, *J Phys. Condens. Matter*, 2012, 24.
50. J. Zhao, C. Yu, N. Wang and H. Liu, *J. Phys. Chem. C*, 2010, 114, 4135-4141.
51. M. Tsutsui, M. Taniguchi and T. Kawai, *J. Am. Chem. Soc.*, 2009, 131, 10552-10556.
52. B. M. Briechle, Y. Kim, P. Ehrenreich, A. Erbe, D. Sysoiev, T. Huhn, U. Groth and E. Scheer, *Beilstein J. Nanotech.*, 2012, 3, 798-808.
53. I. Baldea, *Phys. Rev. B*, 2012, 85.
54. F. Mirjani, J. M. Thijssen and S. J. van der Molen, *Phys. Rev. B*, 2011, 84.
55. M. C. Lennartz, N. Atodiresei, V. Caciuc and S. Karthaeuser, *J. Phys. Chem. C*, 2011, 115, 15025-15030.
56. A. V. Malyshev, *Phys. Rev. Lett.*, 2007, 98.

57. L. Venkataraman, J. E. Klare, C. Nuckolls, M. S. Hybertsen and M. L. Steigerwald, *Nature*, 2006, 442, 904-907.
58. T. Kim, P. Darancet, J. R. Widawsky, M. Kotiuga, S. Y. Quek, J. B. Neaton and L. Venkataraman, *Nano Lett.*, 2014, 14, 794-798.
59. S. Lara-Avila, A. V. Danilov, S. E. Kubatkin, S. L. Broman, C. R. Parker and M. B. Nielsen, *J. Phys. Chem. C*, 2011, 115, 18372-18377.
60. S. Battacharyya, A. Kibel, G. Kodis, P. A. Liddell, M. Gervaldo, D. Gust and S. Lindsay, *Nano Lett.*, 2011, 11, 2709-2714.
61. J. R. Widawsky, P. Darancet, J. B. Neaton and L. Venkataraman, *Nano Lett.*, 2012, 12, 354-358.
62. K. Baheti, J. A. Malen, P. Doak, P. Reddy, S.-Y. Jang, T. D. Tilley, A. Majumdar and R. A. Segalman, *Nano Lett.*, 2008, 8, 715-719.
63. L. Bogani and W. Wernsdorfer, *Nature Mater.*, 2008, 7, 179-186.
64. C. Iacovita, M. V. Rastei, B. W. Heinrich, T. Brumme, J. Kortus, L. Limot and J. P. Bucher, *Phys. Rev. Lett.*, 2008, 101.
65. R. Vincent, S. Klyatskaya, M. Ruben, W. Wernsdorfer and F. Balestro, *Nature*, 2012, 488, 357-360.